Theoretical study of early-time superradiance for atom clouds and arrays

F. Robicheaux *

Department of Physics and Astronomy, Purdue University, West Lafayette, Indiana 47907, USA
and Purdue Quantum Science and Engineering Institute, Purdue University, West Lafayette, Indiana 47907, USA

(Received 1 October 2021; accepted 22 November 2021; published 13 December 2021)

We explore conditions for Dicke superradiance in a cloud of atoms by examining the Taylor series expansion of the photon emission rate at $t = 0$. By defining superradiance as an increasing photon emission rate for $t \sim 0$, we have calculated the conditions for superradiance for a variety of cases. We investigate superradiance as defined for photon emission into all angles as well as directional superradiance where the photon emission is only detected in a particular direction. Although all of the examples are for two-level atoms that are fully inverted at $t = 0$, we also give equations for partially inverted two-level atoms and for fully inverted multilevel atoms. We give an algorithm for efficiently evaluating these equations for atom arrays and determine superradiance conditions for large atom number.

DOI: 10.1103/PhysRevA.104.063706

I. INTRODUCTION

Superradiance [1–4] is a collective phenomenon where multiple atoms radiate faster than N individual atoms due to their interaction through the quantized electromagnetic field. For atoms within a small region, the peak photon emission rate can scale like N^2 rather than N from uncorrelated atoms. This leads to a burst of radiation on a time scale much smaller than the radiative lifetime of a single atom. There has been an extensive number of experimental studies of superradiance in atoms [5–27], investigations of superradiance for a wide variety of other platforms [28–35], and many theoretical investigations of different cases [36–65].

In this paper, we follow the philosophy of Ref. [65] to use the early-time behavior of the photon emission rate to determine whether or not a group of N atoms are superradiant. They used the statistics of the first two photons emitted to classify the system. For this they used the $g^{(2)}(0)$ with the condition that superradiance occurs when the first photon emission enhances the rate of the second photon emission, i.e., $g^{(2)}(0) > 0$. With this insight, they did not need to solve for the time dependence of the master equation to determine superradiance. They classified whether or not a system is superradiant by using the variance of the eigenvalues of the decay matrix, Γ_{nm} in Eq. (6) below, because the $g^{(2)}(0)$ can be found in terms of these values. Also important, this formulation allows for interpretation of results from large systems

Instead of using $g^{(2)}(0)$, in this paper, we use the early-time behavior of the photon emission rate to determine whether or not a system is superradiant. The idea is that the photon emission rate $\gamma(t)$ is an increasing function of time at $t = 0$ when the system is superradiant. Using the criterion $\dot{\gamma}(0) > 0$, we obtain the superradiance condition in terms of the trace of the square of the decay matrix. Because the decay matrix is real and symmetric, this criterion is exactly that of Ref. [65]. An advantage of the new definition is that it is computationally more efficient so that larger systems can be investigated. It also leads to different insight into the conditions for superradiance. Another advantage is that this formulation allows for generalization to multilevel systems, systems that are not fully inverted, directional superradiance, and efficient evaluation for arrays.

In many of the examples below, we emphasize the difference between superradiance as defined from the total emission rate and superradiance as defined as the emission rate into a particular direction. As an example, Ref. [27] experimentally demonstrated cases with clear superradiance in a particular direction (as evidenced by increasing photon emission rate at early time) with no enhancement in other directions and Ref. [64] theoretically investigated directional superradiance for weakly illuminated atom arrays. While the theory can be used for randomly placed atoms, all examples below are for atom arrays. For two- and three-dimensional arrays, we give examples of directional superradiance with atom separations comparable to or larger than the wavelength of the light for experimentally accessible atom numbers. We also take advantage of the efficiency in evaluating $\dot{\gamma}(0)$ to demonstrate its scaling with number of atoms and show that superradiance occurs in two- and three-dimensional atom arrays for sufficient atom number.

In Sec. II, we give the basic theory when the atoms are approximated as two-level systems. In Sec. III, we derive the expressions for the early-time behavior of the photon emission rate for two-level atoms, which can then be used to define superradiance while Sec. IV is the early-time behavior for a specific type of multilevel atom. In Sec. V, we explore several examples. In Sec. VI is a summary of these results. Appendix gives a brief derivation of the equivalence of our superradiance condition with that in Ref. [65].

II. BASIC THEORY: TWO STATES

In this section, we are using an excitation scheme where the atomic structure is approximated as a two-level system.

*robichf@purdue.edu

The atoms will be considered as fixed in space, which means we are ignoring the atom recoil and Doppler effects.

A. Master equation formalism

All of the equations will use a simplified notation to reduce their size. For the nth atom, the ground and excited states are $|g_n\rangle$ and $|e_n\rangle$. The operators used below follow the definition

$$\hat{e}_n \equiv |e_n\rangle\langle e_n| \quad \hat{\sigma}_n^- \equiv |g_n\rangle\langle e_n| \quad \hat{\sigma}_n^+ \equiv |e_n\rangle\langle g_n|. \tag{1}$$

The equation for the N-atom density matrix [66] can be written in the form

$$\frac{d\hat{\rho}}{dt} = \sum_n \left(\mathcal{L}_n(\hat{\rho}) + \sum_{m\neq n} \left[\frac{1}{i\hbar}[H_{nm}, \hat{\rho}] + \mathcal{L}_{nm}(\hat{\rho}) \right] \right), \tag{2}$$

where the one-atom Hamiltonian that arises from an external laser interacting with each atom is zero for all of the examples below and has not been included, $\mathcal{L}_n$ is from one atom decays of Lindblad type, the H_{nm} is the two-atom Hamiltonian from the dipole-dipole interactions, and $\mathcal{L}_{nm}$ are the two atom decays from the dipole-dipole interactions. For the two-level cases considered here, these operators are

$$\mathcal{L}_n(\hat{\rho}) = \frac{\Gamma}{2}(2\hat{\sigma}_n^-\hat{\rho}\hat{\sigma}_n^+ - \hat{e}_n\hat{\rho} - \hat{\rho}\hat{e}_n) \tag{3}$$

$$H_{nm} = \hbar\Omega_{nm}\hat{\sigma}_n^+\hat{\sigma}_m^- \tag{4}$$

$$\mathcal{L}_{nm} = \frac{\Gamma_{nm}}{2}(2\hat{\sigma}_n^-\hat{\rho}\hat{\sigma}_m^+ - \hat{\sigma}_m^+\hat{\sigma}_n^-\hat{\rho} - \hat{\rho}\hat{\sigma}_m^+\hat{\sigma}_n^-), \tag{5}$$

where Γ is the decay rate of a single atom. The two-atom parameters are defined for $m \neq n$ as

$$\Gamma_{nm} = g(\boldsymbol{R}_{nm}) + g^*(\boldsymbol{R}_{nm}) = 2\mathrm{Re}[g(\boldsymbol{R}_{nm})] \tag{6}$$

$$\Omega_{nm} = \frac{g(\boldsymbol{R}_{nm}) - g^*(\boldsymbol{R}_{nm})}{2i} = \mathrm{Im}[g(\boldsymbol{R}_{nm})] \tag{7}$$

$$g(\boldsymbol{R}) = \frac{\Gamma}{2}\left[h_0^{(1)}(s) + \frac{3\hat{R}\cdot\hat{d}^*\hat{R}\cdot\hat{d} - 1}{2} h_2^{(1)}(s) \right] \tag{8}$$

$$g_{nm}^{\pm} \equiv \pm i\Omega_{nm} + \tfrac{1}{2}\Gamma_{nm} \tag{9}$$

with $\boldsymbol{R}_{nm} = \boldsymbol{R}_n - \boldsymbol{R}_m$ with $\boldsymbol{R}_n$ the position of atom n, $\hat{d}$ the dipole unit vector, $s = kR$, $\hat{R} = \boldsymbol{R}/R$, and the $h_\ell^{(1)}(s)$ the outgoing spherical Hankel function of angular momentum ℓ: $h_0^{(1)}(s) = e^{is}/[is]$ and $h_2^{(1)}(s) = (-3i/s^3 - 3/s^2 + i/s)e^{is}$. The $g(\boldsymbol{R})$ is proportional to the propagator that gives the electric field at $\boldsymbol{R}$ given a dipole at the origin [67]. For a $\Delta M = 0$ transition, $\hat{d} = \hat{z}$ and the coefficient of the $h_2^{(1)}$ Bessel function is $P_2[\cos(\theta)] = [3\cos^2(\theta) - 1]/2$ where $\cos(\theta) = Z/R$. For a $\Delta M = \pm 1$ transition, the coefficient of the $h_2^{(1)}$ Bessel function is $-(1/2)P_2[\cos(\theta)] = [1 - 3\cos^2(\theta)]/4$. To simplify some formulas below, we will define the diagonal component of Γ_{mn} as

$$\Gamma_{nn} = 2\Re[g(\boldsymbol{R} \to 0)] = \Gamma. \tag{10}$$

B. Photon emission rate

The rate that photons are emitted into all angles at time t is given by

$$\gamma(t) = \sum_n \left[\Gamma\langle\hat{e}_n\rangle(t) + \sum_{m\neq n} \Gamma_{mn}\langle\hat{\sigma}_m^+\hat{\sigma}_n^-\rangle(t) \right]. \tag{11}$$

The rate that photons are emitted into the $\hat{k}_f$ direction is proportional to [4]

$$\gamma(t, \boldsymbol{k}_f) = \Gamma \sum_n \left[\langle\hat{e}_n\rangle(t) + \sum_{m\neq n} e^{i\varphi_{mn}}\langle\hat{\sigma}_m^+\hat{\sigma}_n^-\rangle(t) \right], \tag{12}$$

where $\varphi_{mn} = \boldsymbol{k}_f \cdot (\boldsymbol{R}_m - \boldsymbol{R}_n)$ with $\boldsymbol{k}_f = 2\pi/\lambda_0 \hat{\boldsymbol{k}}_f$. The normalization of $\gamma(t, \boldsymbol{k}_f)$ was chosen so that a fully inverted system has $\gamma(0, \boldsymbol{k}) = N\Gamma$ in analogy with $\gamma(0)$. The definition Eq. (12) only makes sense if the orientation of the dipoles are not in the $\hat{k}$ direction because the actual directional rate involves the direction of the dipole and the $\hat{k}$.

An interesting question arises from these two definitions. As noted by Ref. [65], a natural definition of superradiance is when the emission of the first photon enhances the rate that the second photon is emitted. This implies the rate of photon emission, Eq. (11), is an increasing function of time at $t = 0$ since an increasing $\gamma(t)$ means the many atoms radiate faster as time develops. This can only occur when pair correlations $\langle\hat{\sigma}_m^+\hat{\sigma}_n^-\rangle(t) \neq 0$ develop in the gas because the $\sum_n\langle\hat{e}_n\rangle$ is a decreasing function of time for undriven atoms. As we will see below and was experimentally observed in Ref. [27], there are cases where $\dot{\gamma}(0, \boldsymbol{k}) > 0$ for some directions $\hat{k}$ even though $\dot{\gamma}(0) < 0$. However, for $\dot{\gamma}(0, \boldsymbol{k}) > 0$, there must be nonzero (and substantial) pair correlations developing in the atom cloud even when $\dot{\gamma}(0) < 0$. We will call this case "directional superradiance" to distinguish it from the case where $\dot{\gamma}(0) > 0$.

Both types of superradiance are interesting because the gas has become correlated. This can be seen from the development of an initially fully inverted system, which has $\langle\hat{\sigma}_n^{\pm}\rangle(t) = 0$. Therefore, superradiance demands $\langle\hat{\sigma}_m^+\hat{\sigma}_n^-\rangle(t) - \langle\hat{\sigma}_m^+\rangle(t)\langle\hat{\sigma}_n^-\rangle(t) \neq 0$ implying non-negligible pair correlations.

C. Uncorrelated initial state

In the following, we will examine how correlations develop when starting from a completely uncorrelated but not necessarily fully inverted initial state

$$|\psi_i\rangle = \Pi_{\otimes n}[\cos(\alpha/2)\,|g_n\rangle + e^{i\boldsymbol{k}_i\cdot\boldsymbol{R}_n}\sin(\alpha/2)\,|e_n\rangle], \tag{13}$$

where $\sin^2(\alpha/2)$ is the probability for an atom to be excited and $\hat{k}_i$ gives a phase change across the atom cloud. This form for the initial state would result when a cloud was subject to an intense but short laser pulse in the limit that the pulse duration gets very short. We will examine superradiance as a function of both α and $\hat{k}_i$. Superradiance can occur when the cloud is not fully inverted. The interplay between $\hat{k}_i$ and the shape of the cloud can lead to interesting effects, e.g., if the cloud is elongated in the $\hat{k}_i$ direction.

III. EVALUATION OF EARLY-TIME PHOTON RATES: TWO STATES

A. First derivative

We will use a somewhat different approach from Ref. [65] to exactly evaluate the early-time behavior of the photon emission rates, γ's. The idea is based on performing a Taylor series expansion

$$\gamma(t) = \gamma(0) + \dot{\gamma}(0)t + \tfrac{1}{2}\ddot{\gamma}(0)t^2 + \cdots, \tag{14}$$

where $\dot{\gamma}(0)$ means the first derivative of γ evaluated at $t = 0$, etc. Superradiance occurs when $\dot{\gamma}(0) > 0$.

The evaluation of $\dot{\gamma}(0)$ simply requires the derivatives of $\langle \hat{e}_n \rangle$ and $\langle \hat{\sigma}_m^+ \hat{\sigma}_n^- \rangle$

$$\frac{d\langle \hat{e}_n \rangle}{dt} = -\Gamma \langle \hat{e}_n \rangle - \sum_{m \neq n} (g_{nm} \langle \hat{\sigma}_m^- \hat{\sigma}_n^+ \rangle + g_{nm}^* \langle \hat{\sigma}_m^+ \hat{\sigma}_n^- \rangle) \tag{15}$$

and

$$\begin{aligned} \frac{d\langle \hat{\sigma}_m^+ \hat{\sigma}_n^- \rangle}{dt} &= -\Gamma \langle \hat{\sigma}_m^+ \hat{\sigma}_n^- \rangle + 2\Gamma_{mn} \langle \hat{e}_m \hat{e}_n \rangle - g_{mn} \langle \hat{e}_m \rangle \\ &\quad - g_{mn}^* \langle \hat{e}_n \rangle + \sum_{l \neq m,n} [g_{nl} (2\langle \hat{\sigma}_l^- \hat{\sigma}_m^+ \hat{e}_n \rangle - \langle \hat{\sigma}_l^- \hat{\sigma}_m^+ \rangle) \\ &\quad + g_{ml}^* (2\langle \hat{\sigma}_l^+ \hat{e}_m \hat{\sigma}_n^- \rangle - \langle \hat{\sigma}_l^+ \hat{\sigma}_n^- \rangle)] \end{aligned} \tag{16}$$

from Ref. [68].

Using the initial wave function, Eq. (13), all of the expectation values can be evaluated at $t = 0$:

$$\langle \hat{e}_n \rangle = \frac{1 - \cos\alpha}{2} \quad \langle \hat{\sigma}_n^- \rangle = \langle \hat{\sigma}_n^+ \rangle^* = \frac{\sin\alpha}{2} e^{i\boldsymbol{k}_i \cdot \boldsymbol{R}_n} \tag{17}$$

with all of the other expectation values being products of these, $\langle \hat{A}\hat{B} \rangle = \langle \hat{A} \rangle \langle \hat{B} \rangle$, since the initial wave function is a product state.

For clarity, we first give the result for a fully inverted gas, $\alpha = \pi$, for the total photon emission rate:

$$\dot{\gamma}(0) = -N\Gamma^2 + \sum_{n,m \neq n} \Gamma_{mn}\Gamma_{nm} = -2N\Gamma^2 + \mathrm{Tr}[\underline{\Gamma}\,\underline{\Gamma}], \tag{18}$$

where $\underline{\Gamma}$ means the matrix of Γ_{mn} and Tr[...] means the trace. This expression arises because $\langle \hat{e}_n \rangle = 1$ and $\langle \hat{\sigma}_n^\pm \rangle = 0$. Because $\underline{\Gamma}$ is a real, symmetric matrix, our condition $\dot{\gamma}(0) > 0$ is identical to Eq. (3) of Ref. [65], which gives the superradiance condition in terms of the variance of the eigenvalues of $\underline{\Gamma}$; see Appendix below. While the form Eq. (3) of Ref. [65] has advantages as discussed there, Eq. (18) has the advantage of being computationally faster (number of operations scaling like N^2 instead of N^3) and providing insight into scaling with large atom numbers (discussed below). Also, as discussed below, the number of operations scales as N^1 for arrays. The Dicke model [1], $\Gamma_{mn} = 1$, in Eq. (18) gives $\dot{\gamma}(0) = N(N-2)\Gamma^2$, which is the result from Dicke's original derivation.

The fully inverted gas for directional emission has

$$\begin{aligned} \dot{\gamma}(0, \boldsymbol{k}_f) &= -2N\Gamma^2 + \Gamma \sum_{mn} \Gamma_{mn} \cos\varphi_{nm} \\ &= -2N\Gamma^2 + \Gamma \mathrm{Tr}[\underline{\Gamma}\,\underline{\cos\varphi}], \end{aligned} \tag{19}$$

where $\varphi_{mn} = \boldsymbol{k}_f \cdot (\boldsymbol{R}_m - \boldsymbol{R}_n)$. Because this expression only has one power of Γ_{mn} (which decreases like $1/|\boldsymbol{R}_m - \boldsymbol{R}_n|$), the condition $\dot{\gamma}(0, \boldsymbol{k}_f) > 0$ can be satisfied more easily than Eq. (18) if the $\boldsymbol{k}_f$ is in the correct direction.

The equations for partially inverted samples are somewhat more complicated due to the survival of terms with raising and lowering operators. The total decay rate gives

$$\begin{aligned} \dot{\gamma}(0) = -N\Gamma^2 \frac{1-c}{2} + \sum_n \sum_{m \neq n} \Bigg[\frac{c(c-1)}{2} \Gamma_{mn}\Gamma_{nm} - \frac{s^2}{2}\Gamma_{mn} \\ \times \left\{ \Gamma \cos(\eta_{mn}) + \frac{c}{2} \sum_{l \neq n,m} \left(g_{nl} e^{i\eta_{lm}} + g_{ml}^* e^{-i\eta_{ln}} \right) \right\} \Bigg], \end{aligned} \tag{20}$$

where $c \equiv \cos\alpha$, $s \equiv \sin\alpha$, and $\eta_{mn} = \mathbf{k}_i \cdot (\mathbf{R}_m - \mathbf{R}_n)$. The directional decay rate is

$$\begin{aligned} \dot{\gamma}(0, \mathbf{k}_f) = -N\Gamma^2 \frac{1-c}{2} + \Gamma \sum_n \sum_{m \neq n} \Bigg[\frac{c(c-1)}{2} \Gamma_{mn} \cos\varphi_{nm} \\ - \frac{s^2}{4} \Bigg\{ \Gamma_{nm} \cos(\eta_{mn}) + \Gamma \cos(\varphi_{mn} - \eta_{mn}) \\ + c e^{i\varphi_{mn}} \sum_{l \neq n,m} e^{i\eta_{mn}} \left(g_{nl} e^{i\eta_{lm}} + g_{ml}^* e^{-i\eta_{ln}} \right) \Bigg\} \Bigg]. \end{aligned} \tag{21}$$

An important point to note for the partial inversion is that the number of operations scales as N^3 so these are more difficult calculations.

B. Second derivative: Fully inverted

The second derivative of the photon emission rates are relatively straightforward to evaluate when the atoms are fully inverted using [68]

$$\frac{d^2\langle \hat{e}_n \rangle}{dt^2}(0) = \Gamma^2 - \sum_{m \neq n} \Gamma_{nm}\Gamma_{mn} \tag{22}$$

and

$$\frac{d^2\langle \hat{\sigma}_m^+ \hat{\sigma}_n^- \rangle}{dt^2}(0) = -4\Gamma\Gamma_{mn} + \sum_{l \neq m,n} (g_{nl}\Gamma_{lm} + g_{ml}^*\Gamma_{ln}). \tag{23}$$

Using these expressions gives

$$\begin{aligned} \ddot{\gamma}(0) &= N\Gamma^3 - 5\Gamma \sum_{nm} (1 - \delta_{nm}) \Gamma_{nm}\Gamma_{mn} \\ &\quad + \sum_{nml} (1 - \delta_{nl})(1 - \delta_{ml})(1 - \delta_{nm}) \Gamma_{nm}\Gamma_{ml}\Gamma_{ln} \\ &= 8N\Gamma^3 - 8\Gamma \mathrm{Tr}[\underline{\Gamma}\,\underline{\Gamma}] + \mathrm{Tr}[\underline{\Gamma}\,\underline{\Gamma}\,\underline{\Gamma}] \end{aligned} \tag{24}$$

for the total decay rate. The Dicke model [1], gives $\ddot{\gamma}(0) = N(N^2 - 8N + 8)\Gamma^3$, which is the result from Dicke's original derivation. For the directional decay rate,

$$\begin{aligned} \ddot{\gamma}(0, \mathbf{k}_f) = 8N\Gamma^3 - 2\Gamma \mathrm{Tr}[\underline{\Gamma}\,\underline{\Gamma}] - 6\Gamma^2 \mathrm{Tr}[\underline{\Gamma}\,\underline{\cos\eta}] \\ + \Gamma \mathrm{Tr}[\underline{\Gamma}\,\underline{\Gamma}\,\underline{\cos\eta}] + \Gamma \mathrm{Tr}(\underline{\sin\eta}\,[\underline{\Gamma}, \underline{\Omega}]). \end{aligned} \tag{25}$$

In principle, this logic can be continued to higher-order derivatives. With higher derivatives, it might be possible to determine the peak fluorescence and the time at which it occurs. The higher derivatives will require larger powers of the $\underline{\Gamma}$, which would be most efficiently evaluated using the diagonalization described in Ref. [65].

IV. EVALUATION OF EARLY-TIME PHOTON RATES: MANY FINAL STATES

This section gives the $\dot{\gamma}(0)$ when the excited state can decay to several final states. To simplify the notation and derivation, we will do the calculation without spin-orbit and hyperfine effects and further assume the initial state has $\ell = 0$. Extending beyond these restrictions does not seem to be qualitatively different. We will denote the principle quantum number of the excited state as α_i and it can decay to many final states with principle quantum number α_f with $\ell_f = 1$. Instead of using m_f, we will use Cartesian orbitals $i = x, y, z$.

The operators will be extended as

$$\hat{\sigma}_n^{\alpha_f i-} \equiv |(\alpha_f i)_n\rangle\langle e_n| \quad \hat{\sigma}_n^{\alpha_f i+} \equiv |e_n\rangle\langle(\alpha_f i)_n| \tag{26}$$

with the $\hat{e}_n$ operator unchanged. Note the condition

$$\hat{\sigma}_n^{\alpha'_f i'+}\hat{\sigma}_n^{\alpha_f i-} = \hat{e}_n\delta_{ii'}\delta_{\alpha_f\alpha'_f}. \tag{27}$$

The Lindblad term, with $n = m$ allowed, is

$$\mathcal{L}(\hat{\rho}) = \frac{1}{3}\sum_{nm\alpha_f ii'}\frac{\Gamma_{nm}^{\alpha_f ii'}}{2}\big(2\hat{\sigma}_n^{\alpha_f i-}\hat{\rho}\hat{\sigma}_m^{\alpha_f i'+} - \hat{\sigma}_m^{\alpha_f i'+}\hat{\sigma}_n^{\alpha_f i-}\hat{\rho} - \hat{\rho}\hat{\sigma}_m^{\alpha_f i'+}\hat{\sigma}_n^{\alpha_f i-}\big), \tag{28}$$

where

$$\Gamma_{nm}^{\alpha_f ii'} = \Gamma_{\alpha_f}\left[j_0(k_{\alpha_f}R) + \frac{3\hat{R}_i\hat{R}_{i'} - 1}{2}j_2(k_{\alpha_f}R)\right] \tag{29}$$

with Γ_{α_f} the total decay rate into state α_f, k_{α_f} the wave number of the photon that transitions from the initial state to the p state α_f, $j_\ell(z)$ the usual spherical Bessel functions, $R = |\mathbf{R}_n - \mathbf{R}_m|$, and $\hat{R} = (\mathbf{R}_n - \mathbf{R}_m)/R$.

Repeating the derivation of the previous section the slope of the photon emission rate can be found. The rate that photons of wave number magnitude k_{α_f} are emitted for a fully inverted system is

$$\gamma_{\alpha_f}(0) = N\Gamma_{\alpha_f}. \tag{30}$$

The slope of the photon emission for a fully inverted system is

$$\dot{\gamma}_{\alpha_f}(0) = -N\Gamma_{\alpha_f}\Gamma + \sum_n\sum_{m\neq n}\frac{1}{9}\sum_{ii'}\left(\Gamma_{nm}^{\alpha_f ii'}\right)^2, \tag{31}$$

where the total decay rate $\Gamma = \sum_{\alpha_f}\Gamma_{\alpha_f}$. Note that the initial slope needs more atoms to have $\dot{\gamma}_{\alpha_f}(0) > 0$ because the negative term is relatively larger: the second term is proportional to $\Gamma_{\alpha_f}^2$ while the first term is proportional to $\Gamma_{\alpha_f}\Gamma$. The second term is proportional to N^2 so adding more atoms in a compact region will lead to superradiance even when $\Gamma \gg \Gamma_{\alpha_f}$, e.g., Rydberg states.

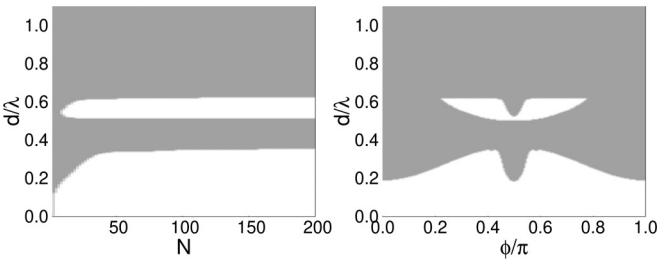

FIG. 1. Both plots are for an atom array in a line on the y axis with the atoms separated by d. The polarization is in the z direction. White shows the region where $\dot{\gamma}(0, \mathbf{k}_f) > 0$ and gray is where <0 with $\mathbf{k}_f = k(\hat{x}\cos\phi + \hat{y}\sin\phi)$. The left plot has $\phi = 0.4\pi$. The right plot is for 100 atoms. For the directional decay, there is more than one region of superradiance unlike the case for $\dot{\gamma}(0)$. For the left plot, the top region only exists for $N \geqslant 9$.

V. EXAMPLES

In this section, we discuss the results of calculations for several examples in one, two, and three dimensions.

A. One-dimensional array

In this section, we describe results for examples where the atoms are in one or two lines with equal spacing between the atoms. Our results for the total decay rate in a one-dimensional atom array match those of Ref. [65] and will not be discussed in detail here. We will mainly focus on the directional photon emission. We will restrict the dipole moment to be in the z direction and the atoms to be on one or two lines parallel to the y axis.

As with Ref. [65], there are regions where the slope of the photon emission rate is larger than 0, indicating superradiance in different directions. After fixing the polarization direction and the line of atoms, there are three parameters of interest: the number of atoms N, the separation of atoms d, and the angle of photon emission. In Fig. 1, we show the region of superradiance as defined by $\dot{\gamma}(0, \mathbf{k}_f) > 0$ for $\mathbf{k}_f = k(\hat{x}\cos\phi + \hat{y}\sin\phi)$. The superradiant region is white. In this case, there is a single line of atoms. One plot shows the superradiant region as a function of N, d for $\phi = 0.4\pi$ and the other shows this region versus ϕ, d for $N = 100$. The plot versus ϕ, d repeats for $\phi \to \phi + \pi$ and is symmetric about $\phi = \pi/2$ due to the symmetry for a line of atoms in the y direction.

As with the results for the total emission rate in Ref. [65], there is a region of relatively rapid change with N for N less than about 20 followed by slower change with N, which apparently converges to particular values for large N. The region of slow increase is discussed in Sec. V D. Unlike the total emission rate, the directional emission has two regions of superradiance for larger N depending on the angle of emission. For ϕ between $\sim\pi/4$ and $\sim 3\pi/4$, there is a region of larger separation, d/λ roughly between 0.5 and 0.6, where the photoemission rate increases with time at early times. This is due to constructive interference in these directions and is not present for the total emission rate, which is only superradiant for d less than $\simeq \lambda/4$ for $N = 100$. This region of directional superradiance for $d \sim \lambda/2$ is only present for

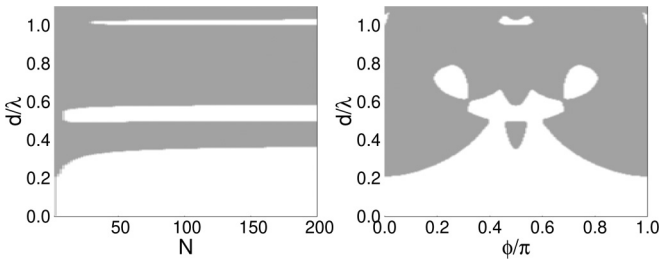

FIG. 2. Same situation as Fig. 1, except there are two lines of atoms, each with $N/2$ atoms. The lines of atoms are displaced from each other by d in the x direction. For the left plot, $\phi = 0.5\pi$. The middle region of superradiance only exists for $N \geqslant 9$ and the top region only exists for $N \geqslant 30$. Note the top region is superradiant for d larger than λ.

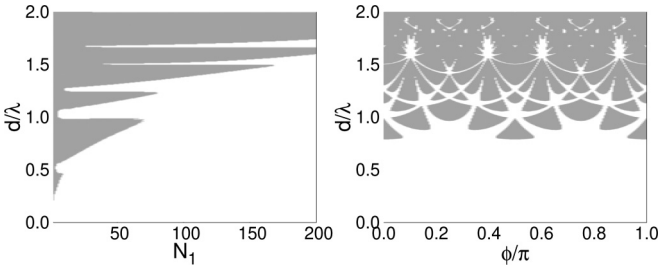

FIG. 3. Same situation as Fig. 1, except there is a square array of atoms in the xy plane of size $N_1 \times N_1$. The dipole moment is perpendicular to the plane and $\mathbf{k}_f = k(\hat{x}\cos\phi + \hat{y}\sin\phi)$. For the left plot, $\phi = 0$ and the right plot has $N_1 = 40$.

$N \geqslant 9$, which is not a large number of atoms. It seems possible to experimentally observe this directional superradiance at larger d.

A more complex situation occurs if there are two, parallel lines of atoms. Figure 2 shows results when the second line of atoms is displaced in the x direction by d. Each line contains $N/2$ atoms. For this case, one plot shows the superradiant region as a function of N, d for $\phi = \pi/2$ and the other shows this region versus ϕ, d for $N = 100$. There are two interesting differences from the example with one line of atoms. The first is that there are more regions of directional superradiance. For $\phi = \pi/2$, there are three regions with the middle region starting at $N = 9$ and the top region starting at $N = 30$. For larger N, there is a rich structure of superradiance on the ϕ, d plane due to the interference between the different lines of atoms. The second is that there is directional superradiance for $d > \lambda$ for $\phi \simeq 0, \pi/2, \pi$. This region of superradiance for $d > \lambda$ requires more atoms, but N is not so large that it is out of reach for experimental investigation.

1. Nonideal cases

For the cases in Figs. 1 and 2, we calculated the effect of not fully inverting the atoms for $N = 100$ for $d < 1.1\lambda$. For this case, we assumed the laser propagation is in the z direction giving $\eta_{mn} = 0$. As α decreases from π, the region of superradiance shrinks. When the excited population decreases too much, the superradiance regions for larger d, i.e., $d \sim \lambda/2$ for Fig. 1 and $d \sim \lambda/2$ and $\sim\lambda$ for Fig. 2, disappear. For the single line case, the upper region disappears when the initial excitation population decreases below 75%. For the double line case, the region near $d \sim \lambda$ disappears for less than approximately 80% excited while the region near $d \sim \lambda/2$ survives down to approximately 55% excited.

Another possible nonideal case has the atoms fully inverted but some of the atoms are randomly removed, which was treated in Ref. [65]. We simulated this by randomly removing each atom with a probability, P. For each P, we repeated the simulations 100 times and checked the superradiance condition. As with the non-fully-inverted case, the region of superradiance shrinks with increasing probability for atom removal and at some point the superradiance regions for larger d disappear. For the single line case, the upper region disappears on average when the number of atoms is less than 80% while for the double line case the region near $d \sim \lambda$ disappears for less than 70% atoms while the region near $d \sim \lambda/2$ survives down to approximately 40% atoms. Similar behavior is seen for higher-dimensional arrays.

B. Two-dimensional array

In this section, we describe results for an example where the atoms are in a two-dimensional array with equal spacing between the atoms. Our results for the total decay rate in a two-dimensional atom array match those of Ref. [65]; we discuss these results below with those from a cubic array. We restrict the dipole moment to be in the z direction and the atoms to be on a square array in the xy plane of size $N_1 \times N_1$.

In Fig. 3, we show the superradiant region versus N_1, d for $\phi = 0$ and versus ϕ, d for $N_1 = 40$ corresponding to $N = 1600$ atoms. As with the results for the total emission rate in Ref. [65], there is a region of relatively rapid change with N_1 for N_1 less than about 20 followed by slower change with N_1. The change was even slower in the plots of Ref. [65] because the plots were versus the total number of atoms $N = N_1^2$, which greatly stretches the abscissa. Unlike the one-dimensional case, it is not clear whether the superradiant regions converge with increasing N_1. It appears that the separation of atoms leading to superradiance increases as the number of atoms increases. This is discussed in Sec. V D where it is shown the results do not converge with increasing N.

The directional superradiance for a plane is much richer than that for one or two lines of atoms. In the plot versus ϕ, d at $N_1 = 40$, the results repeat for $\phi \to \phi + \pi/2$ and are symmetric about $\phi = \pi/4$ and $3\pi/4$ because of the symmetry for a square array. In addition, there are many more regions of superradiance due to the different possible directions for constructive interference. Some of these regions start at relatively small N_1. For example, the superradiant region for $d \sim \lambda$ for $\phi = 0$ starts at $N_1 = 6$ corresponding to 36 atoms. The superradiant region for $d \sim 5\lambda/4$ starts for $N_1 = 11$ corresponding to 121 atoms. Both of these cases are within current experimental capabilities [69]. Perhaps even more interesting are the regions where different constructive interference conditions overlap, for example, the regions for $d \sim 1.6\lambda$ for $\phi \sim \pi/8, 3\pi/8, 5\pi/8, 7\pi/8$. Also of interest are the superradiant regions where $d \sim 2\lambda$; however, these regions are small and may not be robust to lattice imperfections.

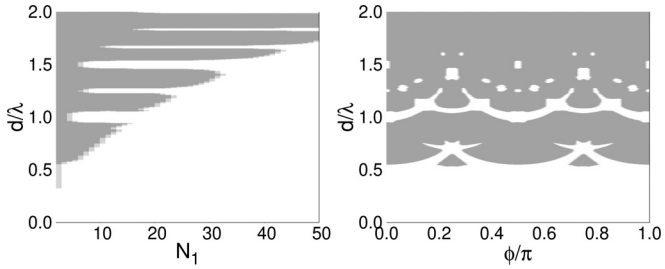

FIG. 4. Same situation as Fig. 1, except there is a cubic array of atoms of size $N_1 \times N_1 \times N_1$. The dipole moment is in the z direction and $\mathbf{k}_f = k(\hat{x}\cos\phi + \hat{y}\sin\phi)$. For the left plot, $\phi = 0$ and the right plot has $N_1 = 10$.

C. Three-dimensional array

In this section, we describe results for an example where the atoms are in a three-dimensional array with equal spacing between the atoms. We restrict the dipole moment to be in the z direction and the atoms to be on a cubic array of size $N_1 \times N_1 \times N_1$.

We will first examine the case for directional superradiance. In Fig. 4, we show the superradiant region versus N_1, d for $\phi = 0$ and versus ϕ, d for $N_1 = 10$ corresponding to $N = 1000$ atoms. As with the planar array, there is a richness to the regions that arise due to directions giving constructive interference. As with the planar array, in the plot versus ϕ, d at $N_1 = 10$, the results repeat for $\phi \to \phi + \pi/2$ and are symmetric about $\phi = \pi/4$ and $3\pi/4$ because of the symmetry for a cubic array. There are also several regions that are superradiant for d greater than $\sim\lambda$ for relatively small number of atoms. Another interesting similarity to the two-dimensional case is the increasing separation of atoms leading to superradiance as the number atoms increases. This is discussed in Sec. V D where it is shown the results do not converge with N.

We also show the superradiant region for total photon emission, $\dot{\gamma}(0)$, versus N_1, d for the square and cubic arrays in Fig. 5. For the square array, the region for $N_1 \leqslant 40$ matches that shown in Ref. [65], Fig. 4, for the polarization perpendicular to the plane. Interestingly, the maximum d for superradiance appears to be an increasing function of N_1 up to the largest values shown in Fig. 5. From Eq. (37), the maximum d/λ for superradiance is proportional to $\sqrt{\ln N_1}$, which does continue to increase with N_1, albeit slowly. For the cubic array, there are more regions of large separation superradiance and they appear at smaller N_1. This is not surprising because

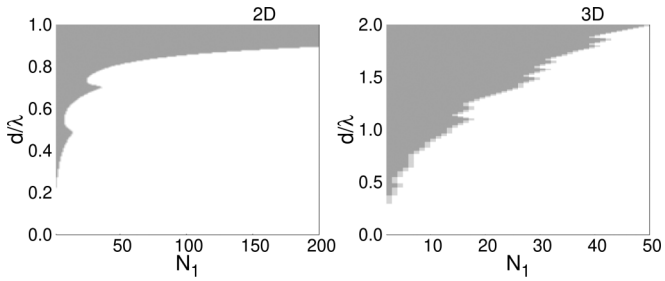

FIG. 5. For the same case as Figs. 3 (for 2D) and 4 (for 3D), plots of the superradiant region defined by $\dot{\gamma}(0) > 0$.

there are many more atoms close to each other, which leads to faster radiation. More interesting, from Eq. (38), the maximum d/λ for superradiance is proportional to $\sqrt{N_1}$. Unlike the one-dimensional case, the two- and three-dimensional arrays do not converge to superradiance properties as N_1 increases.

D. Efficient summation and asymptotic trends

The summation in Eqs. (18) and (19) require $O(N^2)$ operations for a general positioning of atoms. While this is more efficient than $O(N^3)$ operations, there are more efficient algorithms in some cases. For example, for an array, most of the terms are repeated. This fact can be used to reduce the number of operations to $O(N)$.

For a single line, there are N terms where $n - m = 0$; there are $N - 1$ terms where $n - m = 1$ or $n - m = -1$, etc. This allows the calculation in terms of the difference in positions and a weight for a given difference. As another example, for a three-dimensional array with N_1 points in each direction with lattice vectors $\mathbf{a}_1, \mathbf{a}_2, \mathbf{a}_3$ the atom positions can be written as $\mathbf{R}_n = \nu_{1,n}\mathbf{a}_1 + \nu_{2,n}\mathbf{a}_2 + \nu_{3,n}\mathbf{a}_3$ where the $1 \leqslant \nu_1, \nu_2, \nu_3 \leqslant N_1$ are integers. There are $\prod_i (N_1 - |\nu_i|)$ terms that have $\nu_{1,n} - \nu_{1,m} = \nu_1$, $\nu_{2,n} - \nu_{2,m} = \nu_2$, and $\nu_{3,n} - \nu_{3,m} = \nu_3$. Defining the scaled initial slope of the photoemission rate as $\dot{\gamma}(0)/(N\Gamma^2)$, this allows the reduction to

$$\frac{\dot{\gamma}(0)}{N\Gamma^2} = -2 + \sum_{\nu_1\nu_2\nu_3} W_{\nu_1\nu_2\nu_3} \frac{\Gamma^2_{\nu_1\nu_2\nu_3}}{\Gamma^2} \tag{32}$$

$$\frac{\dot{\gamma}(0, \mathbf{k}_f)}{N\Gamma^2} = -2 + \sum_{\nu_1\nu_2\nu_3} W_{\nu_1\nu_2\nu_3} \frac{\Gamma_{\nu_1\nu_2\nu_3}}{\Gamma} \cos\left(\phi_{\nu_1\nu_2\nu_3}\right) \tag{33}$$

$$W_{\nu_1\nu_2\nu_3} = \left(1 - \frac{|\nu_1|}{N_1}\right)\left(1 - \frac{|\nu_2|}{N_1}\right)\left(1 - \frac{|\nu_3|}{N_1}\right), \tag{34}$$

where both summations are for $-N_1 < \nu_1, \nu_2, \nu_3 < N_1$, the number of atoms $N = N_1^3$, $\phi_{\nu_1\nu_2\nu_3} = \mathbf{k}_f \cdot (\nu_1\mathbf{a}_1 + \nu_2\mathbf{a}_2 + \nu_3\mathbf{a}_3)$, and $\Gamma_{\nu_1\nu_2\nu_3} = 2\mathrm{Re}[g(\nu_1\mathbf{a}_1 + \nu_2\mathbf{a}_2 + \nu_3\mathbf{a}_3)]$. The function $W_{\nu_1\nu_2\nu_3}$ is the weighting from the number of terms with differences ν_1, ν_2, ν_3. The extension to one- and two-dimensional arrays is straightforward: restrict $\nu_2 = \nu_3 = 0$ in one dimension and restrict $\nu_3 = 0$ in two dimensions.

This formulation, Eqs. (32) and (33), shows why the one-dimensional case converges to a finite value in the limit $N \to \infty$. The scaled initial slope of the photoemission rate goes to an asymptotic limit as $N \to \infty$:

$$\lim_{N\to\infty} \frac{\dot{\gamma}(0)}{N\Gamma^2} = -2 + \sum_{\nu=-\infty}^{\infty} \frac{\Gamma_\nu^2}{\Gamma^2} \tag{35}$$

$$\lim_{N\to\infty} \frac{\dot{\gamma}(0, \mathbf{k}_f)}{N\Gamma^2} = -2 + \sum_{\nu=-\infty}^{\infty} \frac{\Gamma_\nu}{\Gamma} \cos(\phi_\nu). \tag{36}$$

The first summation is absolutely convergent because Γ_ν^2 is proportional to $1/\nu^2$ for large $|\nu|$. The second summation is conditionally convergent because $\Gamma_\nu \cos(\phi_\nu)$ is proportional to $1/|\nu|$ times an oscillating function of ν for large $|\nu|$.

From the formulation, Eqs. (32) and (33), we can show the two-dimensional case always leads to superradiance in the limit $N \to \infty$. For example, in Eq. (32), the sum diverges proportional to $\ln N_1$ because the $\Gamma_{\nu_1\nu_2} \propto 1/|\mathbf{a}_1\nu_1 + \mathbf{a}_2\nu_2|$. As

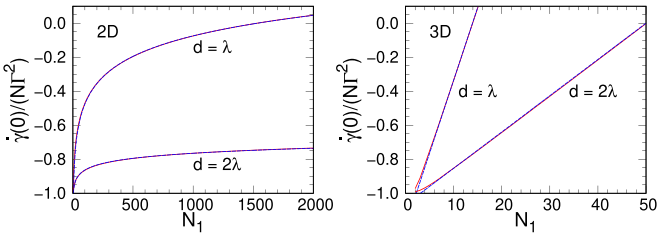

FIG. 6. For the same case as Figs. 3 and 4, a plot of the scaled initial slope of total radiation at a separation $d = \lambda$ and 2λ versus the number of atoms in each direction. The red solid line is the calculation using Eq. (32) and the blue dashed line is a plot of $-1.2762 + 0.1740 \ln N_1$ and $-1.0608 + 0.0429 \ln N_1$ for two-dimensional and $-1.1913 + 0.0856 N_1$ and $-1.0608 + 0.0213 N_1$ for three-dimensional. The plane of atoms with polarization perpendicular to the plane is superradiant for $N_1 > 1530$ for $d = \lambda$ while the cubic array is superradiant for $N_1 \geqslant 14$.

a specific example, a square array with separation d and polarization out of the plane gives

$$\frac{\dot\gamma(0)}{N\Gamma^2} \sim C + \frac{9\lambda^2}{32\pi^2 d^2} \sum \frac{W_{\nu_1\nu_2}}{\nu_1^2 + \nu_2^2} \sim C + D\frac{\lambda^2}{d^2} \ln N_1 \quad (37)$$

in the limit of large N_1 with C and D constants. The asymptotic form was found by converting the sum to an integral using $\nu^2 = \nu_1^2 + \nu_2^2$ with $\sum \to \int 2\pi\nu d\nu$. This can be seen in Fig. 6 where we plot the scaled photon emission slope versus N_1. There is a fit function, which agrees well with the calculation with the fit being $-1.2762 + 0.1740 \ln N_1$ for $d = \lambda$ and $-1.0608 + 0.0429 \ln N_1$ for $d = 2\lambda$. This agrees better with Eq. (37) than might be expected given the contribution from the weight function, $9/(16\pi) = 0.1790$.

Unlike the one-dimensional case where the scaled slope converges to a finite value as $N \to \infty$, the two-dimensional scaled slope diverges for both Eqs. (32) and (33) implying there is always a minimum number of atoms, which will give superradiance. For Fig. 6, superradiance occurs for $N_1 \simeq 1530$ corresponding to 2.3×10^6 atoms for $d = \lambda$ and $N_1 \sim 5.5 \times 10^{10}$ corresponding to $N \sim 3 \times 10^{21}$ atoms for $d = 2\lambda$. These are very large numbers, not likely to be accessible experimentally in the near future. The smallest N_1 for superradiance is a rapidly increasing function of d: roughly N_1 is squared for every increase of d by a factor of $\sim\sqrt{2}$. Also, the approximations in the basic equations, Eq. (2), no longer hold when the array size is too large so this asymptotic behavior only represents reality for a finite range of N_1.

From the formulation, Eqs. (32) and (33), we can show that the three-dimensional case always leads to superradiance in the limit $N \to \infty$. Following the logic of the two-dimensional case, the cubic array in x, y, z with separation d and polarization in the z direction gives

$$\frac{\dot\gamma(0)}{N\Gamma^2} \sim C + D\frac{\lambda^2}{d^2} N_1 \quad (38)$$

in the limit of large N_1 with C and D constants. The asymptotic form was found by converting the sum to an integral using $\nu^2 = \nu_1^2 + \nu_2^2 + \nu_3^2$ with $\sum \to \int 4\pi\nu^2 d\nu$. This form can be seen in Fig. 6 where we plot the scaled photon emission slope versus N_1. For N_1 greater than about 4, the scaled photoemission slope is proportional to N_1. There is a fit function, which agrees well with the scaling with the fit being $-1.1913 + 0.0856 N_1$ for $d = \lambda$ and $-1.0608 + 0.0213 N_1$ for $d = 2\lambda$. Note that the coefficient multiplying the N_1 decreases by a factor of 4 in going from $d = \lambda$ to 2λ as expected from Eq. (38).

Because the $\dot\gamma(0)/N$ increases more quickly with N_1 than the two-dimensional case, the region of superradiance is reached more quickly. For $d = \lambda$, there is superradiance for $N_1 \geqslant 14$ (corresponding to $N = 2744$) and, for $d = 2\lambda$, it is $N_1 \geqslant 51$ (corresponding to $N = 130\,000$). Compared to the two-dimensional case, these are much smaller cutoff numbers although they are probably still experimentally challenging in the near future. The form of Eq. (38) suggests that the cutoff for superradiance is $N_1 = N^{1/3} \propto (d/\lambda)^2$.

VI. SUMMARY

We have presented an alternative method to Ref. [65] for determining whether a collection of atoms will exhibit superradiance in the total emission rate. Our condition is equivalent to that in Ref. [65] but uses the trace of the square of a matrix instead of the variance of the eigenvalues. We also presented a method for determining whether the collection of atoms will exhibit superradiance only in particular directions. In addition to expressions for fully inverted systems, we also found expressions for when the gas is partially inverted in a product state. For the case of fully inverted atoms, we determined the condition for superradiance for photoemission into more than one final state. Finally, we showed how to efficiently evaluate these expressions for arrays of atoms and determined the superradiance condition for very large atom number.

For two-level atoms, we performed calculations for directional superradiance for one-, two-, and three-dimensional arrays and found conditions of superradiance where the atom separation was comparable to or larger than λ for not very large numbers of atoms. We showed that one-dimensional arrays have radiant properties that converge to finite values as the number of atoms increase, but two- and three-dimensional arrays have scaled radiant properties that increase with increasing number of atoms. For fully inverted atoms, we showed how the decay into many final states affects the superradiance condition for the total emission rate.

While it will be difficult experimentally to have large, perfect arrays, experiments with randomly situated atoms can be done. Effects that result from the interference due to the perfect array will not be reproduced in a random gas. However, the dependence of the total photon emission rate with d/λ, d the average separation, and atom number, N, should be similar to that for a perfect array when N is large. For example, an effectively two-dimensional cloud should have the scaled initial slope, $\dot\gamma(0)/(N\Gamma^2)$, scale like Eq. (37) and a three-dimensional cloud should scale like Eq. (38). They should scale like the perfect arrays because the main contribution comes from atoms with separations $d \gg \lambda$ where Γ^2_{nm} does not vary strongly when averaged over a wavelength. This suggests that two- and three-dimensional gases also should show superradiance and directional superradiance for enough atoms.

Data used in this publication is available at Ref. [70].

Note added. Recently, we became aware of related work in Ref. [71].

ACKNOWLEDGMENT

This work was supported by the National Science Foundation under Grant No. 2109987-PHY.

APPENDIX: EQUIVALENCE OF SUPERRADIANCE DEFINITION

This Appendix shows that the condition $g^{(2)}(0) > 1$ of Ref. [65] is the same as $\dot{\gamma}(0) > 0$ from Eq. (18). From Eq. (12) in Appendix B of Ref. [65], the superradiance condition is

$$\sum_{\nu=1}^{N} \Gamma_\nu^2 - 2N\Gamma^2 > 0 \tag{A1}$$

with Γ_ν the eigenvalues of $\underline{\Gamma}$. Since $\underline{\Gamma}$ is a real, symmetric matrix, the sum of the squares of the eigenvalues can be related to the trace of the squared matrix:

$$\sum_{\nu=1}^{N} \Gamma_\nu^2 = \mathrm{Tr}[\underline{\Gamma}\ \underline{\Gamma}]. \tag{A2}$$

Substituting this expression into Eq. (A1) immediately gives

$$\mathrm{Tr}[\underline{\Gamma}\ \underline{\Gamma}] - 2N\Gamma^2 = \dot{\gamma}(0) > 0. \tag{A3}$$

[1] R. H. Dicke, Coherence in spontaneous radiation processes, Phys. Rev. **93**, 99 (1954).

[2] N. E. Rehler and J. H. Eberly, Superradiance, Phys. Rev. A **3**, 1735 (1971).

[3] M. Gross and S. Haroche, Superradiance: An essay on the theory of collective spontaneous emission, Phys. Rep. **93**, 301 (1982).

[4] L. Allen and J. H. Eberly, *Optical Resonance and Two-Level Atoms* (Courier Corporation, Mineola, 1987), Vol. 28.

[5] N. Skribanowitz, I. P. Herman, J. C. MacGillivray, and M. S. Feld, Observation of Dicke Superradiance in Optically Pumped HF Gas, Phys. Rev. Lett. **30**, 309 (1973).

[6] M. Gross, C. Fabre, P. Pillet, and S. Haroche, Observation of Near-Infrared Dicke Superradiance on Cascading Transitions in Atomic Sodium, Phys. Rev. Lett. **36**, 1035 (1976).

[7] H. M. Gibbs, Q. H. F. Vrehen, and H. M. J. Hikspoors, Single-Pulse Superfluorescence in Cesium, Phys. Rev. Lett. **39**, 547 (1977).

[8] J. Marek, Observation of superradiance in Rb vapour, J. Phys. B **12**, L229 (1979).

[9] M. Gross, P. Goy, C. Fabre, S. Haroche, and J. M. Raimond, Maser Oscillation and Microwave Superradiance in Small Systems of Rydberg Atoms, Phys. Rev. Lett. **43**, 343 (1979).

[10] A Crubellier, S Liberman, P Pillet, and MG Schweighofer, Experimental study of quantum fluctuations of polarisation in superradiance, J. Phys. B **14**, L177 (1981).

[11] L. Moi, P. Goy, M. Gross, J. M. Raimond, C. Fabre, and S. Haroche, Rydberg-atom masers. I. a theoretical and experimental study of super-radiant systems in the millimeter-wave domain, Phys. Rev. A **27**, 2043 (1983).

[12] T. Wang, S. F. Yelin, R. Côté, E. E. Eyler, S. M. Farooqi, P. L. Gould, M. Koštrun, D. Tong, and D. Vrinceanu, Superradiance in ultracold Rydberg gases, Phys. Rev. A **75**, 033802 (2007).

[13] S. Slama, S. Bux, G. Krenz, C Zimmermann, and Ph. W. Courteille, Superradiant Rayleigh Scattering and Collective Atomic Recoil Lasing in a Ring Cavity, Phys. Rev. Lett. **98**, 053603 (2007).

[14] J. O. Day, E. Brekke, and T. G. Walker, Dynamics of low-density ultracold Rydberg gases, Phys. Rev. A **77**, 052712 (2008).

[15] M. Chalony, R. Pierrat, D. Delande, and D. Wilkowski, Coherent flash of light emitted by a cold atomic cloud, Phys. Rev. A **84**, 011401(R) (2011).

[16] A. Goban, C.-L. Hung, J. D. Hood, S.-P. Yu, J. A. Muniz, O. Painter, and H. J. Kimble, Superradiance for Atoms Trapped Along a Photonic Crystal Waveguide, Phys. Rev. Lett. **115**, 063601 (2015).

[17] T. Zhou, B. G. Richards, and R. R. Jones, Absence of collective decay in a cold Rydberg gas, Phys. Rev. A **93**, 033407 (2016).

[18] W. Guerin, M. O. Araújo, and R. Kaiser, Subradiance in a Large Cloud of Cold Atoms, Phys. Rev. Lett. **116**, 083601 (2016).

[19] S. J. Roof, K. J. Kemp, M. D. Havey, and I. M. Sokolov, Observation of Single-Photon Superradiance and the Cooperative Lamb Shift in an Extended Sample of Cold Atoms, Phys. Rev. Lett. **117**, 073003 (2016).

[20] M. O. Araújo, I. Krešić, R. Kaiser, and W. Guerin, Superradiance in a Large and Dilute Cloud of Cold Atoms in the Linear-Optics Regime, Phys. Rev. Lett. **117**, 073002 (2016).

[21] M. A. Norcia and J. K. Thompson, Cold-Strontium Laser in the Superradiant Crossover Regime, Phys. Rev. X **6**, 011025 (2016).

[22] D. D. Grimes, S. L. Coy, T. J. Barnum, Y. Zhou, S. F. Yelin, and R. W. Field, Direct single-shot observation of millimeter-wave superradiance in Rydberg-Rydberg transitions, Phys. Rev. A **95**, 043818 (2017).

[23] P. Solano, P. Barberis-Blostein, F. K. Fatemi, L. A. Orozco, and S. L. Rolston, Super-radiance reveals infinite-range dipole interactions through a nanofiber, Nature Commun. **8**, 1857 (2017).

[24] L. Chen, P. Wang, Z. Meng, L. Huang, H. Cai, D.-W. Wang, S.-Y. Zhu, and J. Zhang, Experimental Observation of One-Dimensional Superradiance Lattices in Ultracold Atoms, Phys. Rev. Lett. **120**, 193601 (2018).

[25] T. Laske, H. Winter, and A. Hemmerich, Pulse Delay Time Statistics in a Superradiant Laser with Calcium Atoms, Phys. Rev. Lett. **123**, 103601 (2019).

[26] S. J. Masson, I. Ferrier-Barbut, L. A. Orozco, A. Browaeys, and A. Asenjo-Garcia, Many-Body Signatures of Collective Decay in Atomic Chains, Phys. Rev. Lett. **125**, 263601 (2020).

[27] G. Ferioli, A. Glicenstein, F. Robicheaux, R. T. Sutherland, A. Browaeys, and I. Ferrier-Barbut, Laser driven

superradiant ensembles of two-level atoms near Dicke's regime, arXiv:2107.13392.
[28] R. Monshouwer, M. Abrahamsson, F. Van Mourik, and R. Van Grondelle, Superradiance and exciton delocalization in bacterial photosynthetic light-harvesting systems, J. Phys. Chem. B **101**, 7241 (1997).
[29] M. Scheibner, T. Schmidt, L. Worschech, A. Forchel, G. Bacher, T. Passow, and D. Hommel, Superradiance of quantum dots, Nature Phys. **3**, 106 (2007).
[30] R. Röhlsberger, K. Schlage, B. Sahoo, S. Couet, and R. Rüffer, Collective Lamb shift in single-photon superradiance, Science **328**, 1248 (2010).
[31] K. Cong, Q. Zhang, Y. Wang, G. T. Noe, A. Belyanin, and J. Kono, Dicke superradiance in solids, J. Opt. Soc. Am. B **33**, C80 (2016).
[32] R. A. Molina, E. Benito-Matias, A. D. Somoza, L. Chen, and Y. Zhao, Superradiance at the localization-delocalization crossover in tubular chlorosomes, Phys. Rev. E **93**, 022414 (2016).
[33] C. Bradac, M. T. Johnsson, M. van Breugel, B. Q. Baragiola, R. Martin, M. L. Juan, G. K. Brennen, and T. Volz, Room-temperature spontaneous superradiance from single diamond nanocrystals, Nature Commun. **8**, 1205 (2017).
[34] G. Rainò, M. A. Becker, M. I. Bodnarchuk, R. F. Mahrt, M. V. Kovalenko, and T. Stöferle, Superfluorescence from lead halide perovskite quantum dot superlattices, Nature (London) **563**, 671 (2018).
[35] A. Gover, R. Ianconescu, A. Friedman, C. Emma, N. Sudar, P. Musumeci, and C. Pellegrini, Superradiant and stimulated-superradiant emission of bunched electron beams, Rev. Mod. Phys. **91**, 035003 (2019).
[36] R. Friedberg, S. R. Hartmann, and J. T. Manassah, Limited superradiant damping of small samples, Phys. Lett. A **40**, 365 (1972).
[37] R. Friedberg and S. R. Hartmann, Temporal evolution of superradiance in a small sphere, Phys. Rev. A **10**, 1728 (1974).
[38] J. C. MacGillivray and M. S. Feld, Theory of superradiance in an extended, optically thick medium, Phys. Rev. A **14**, 1169 (1976).
[39] F. C. Spano and S. Mukamel, Superradiance in molecular aggregates, J. Chem. Phys. **91**, 683 (1989).
[40] S. John and T. Quang, Localization of Superradiance Near a Photonic Band Gap, Phys. Rev. Lett. **74**, 3419 (1995).
[41] H. J. Carmichael and K. Kim, A quantum trajectory unraveling of the superradiance master equation, Opt. Commun. **179**, 417 (2000).
[42] J. P. Clemens, L. Horvath, B. C. Sanders, and H. J. Carmichael, Collective spontaneous emission from a line of atoms, Phys. Rev. A **68**, 023809 (2003).
[43] M. O. Scully, E. S. Fry, C. H. Raymond Ooi, and K. Wódkiewicz, Directed Spontaneous Emission from an Extended Ensemble of *n* Atoms: Timing is Everything, Phys. Rev. Lett. **96**, 010501 (2006).
[44] A. Svidzinsky and J.-T. Chang, Cooperative spontaneous emission as a many-body eigenvalue problem, Phys. Rev. A **77**, 043833 (2008).
[45] E. Akkermans, A. Gero, and R. Kaiser, Photon Localization and Dicke Superradiance in Atomic Gases, Phys. Rev. Lett. **101**, 103602 (2008).
[46] A. A. Svidzinsky, J.-T. Chang, and M. O. Scully, Cooperative spontaneous emission of *n* atoms: Many-body eigenstates, the effect of virtual Lamb shift processes, and analogy with radiation of *n* classical oscillators, Phys. Rev. A **81**, 053821 (2010).
[47] K. Baumann, C. Guerlin, F. Brennecke, and T. Esslinger, Dicke quantum phase transition with a superfluid gas in an optical cavity, Nature (London) **464**, 1301 (2010).
[48] G.-D. Lin and S. F. Yelin, Superradiance in spin-*j* particles: Effects of multiple levels, Phys. Rev. A **85**, 033831 (2012).
[49] X. Kong and A. Pálffy, Collective radiation spectrum for ensembles with Zeeman splitting in single-photon superradiance, Phys. Rev. A **96**, 033819 (2017).
[50] P. Kirton and J. Keeling, Suppressing and Restoring the Dicke Superradiance Transition by Dephasing and Decay, Phys. Rev. Lett. **118**, 123602 (2017).
[51] R. T. Sutherland and F. Robicheaux, Superradiance in inverted multilevel atomic clouds, Phys. Rev. A **95**, 033839 (2017).
[52] F. Cottier, R. Kaiser, and R. Bachelard, Role of disorder in super- and subradiance of cold atomic clouds, Phys. Rev. A **98**, 013622 (2018).
[53] P. Kirton and J. Keeling, Superradiant and lasing states in driven-dissipative Dicke models, New J. Phys. **20**, 015009 (2018).
[54] P. Kirton, M. M. Roses, J. Keeling, and E. G. Dalla Torre, Introduction to the Dicke model: From equilibrium to nonequilibrium, and vice versa, Adv. Quan. Tech. **2**, 1800043 (2019).
[55] L. Ostermann, C. Meignant, C. Genes, and H. Ritsch, Super-and subradiance of clock atoms in multimode optical waveguides, New J. Phys. **21**, 025004 (2019).
[56] R. T. Sutherland, Analog quantum simulation of superradiance and subradiance in trapped ions, Phys. Rev. A **100**, 061405(R) (2019).
[57] P. Stránský and P. Cejnar, Superradiance in finite quantum systems randomly coupled to continuum, Phys. Rev. E **100**, 042119 (2019).
[58] K. C. Stitely, S. J. Masson, A. Giraldo, B. Krauskopf, and S. Parkins, Superradiant switching, quantum hysteresis, and oscillations in a generalized Dicke model, Phys. Rev. A **102**, 063702 (2020).
[59] D. Das, B. Lemberger, and D. D. Yavuz, Subradiance and superradiance-to-subradiance transition in dilute atomic clouds, Phys. Rev. A **102**, 043708 (2020).
[60] S. Calegari, A. C. Lourenço, G. T. Landi, and E. I. Duzzioni, Genuine multipartite correlations in Dicke superradiance, Phys. Rev. A **101**, 052310 (2020).
[61] S. Fuchs, A. Vukics, and S. Y. Buhmann, Superradiance from nonideal initial states: A quantum trajectory approach, Phys. Rev. A **103**, 043712 (2021).
[62] B. Lemberger and K. Mølmer, Radiation eigenmodes of Dicke superradiance, Phys. Rev. A **103**, 033713 (2021).
[63] R. A. Dourado and M. H. Y. Moussa, Coherent many-body Rabi oscillations via superradiance and superabsorption and the mean-field approach for a superradiant laser, Phys. Rev. A **104**, 023708 (2021).
[64] R. Holzinger, M. Moreno-Cardoner, and H. Ritsch, Nanoscale continuous quantum light sources based on driven dipole emitter arrays, Appl. Phys. Lett. **119**, 024002 (2021).

[65] S. J. Masson and A. Asenjo-Garcia, Universality of Dicke superradiance in arrays of quantum emitters, arXiv:2106.02042.
[66] R. Loudon, *The Quantum Theory of Light, 3rd Edition* (Oxford University Press, New York, 2000).
[67] J. D. Jackson, *Classical Electrodynamics*, 3rd Edition (John Wiley & Sons, New York, 1999).
[68] F. Robicheaux and D. A. Suresh, Beyond lowest order mean-field theory for light interacting with atom arrays, Phys. Rev. A **104**, 023702 (2021).
[69] J. Rui, D. Wei, A. Rubio-Abadal, S. Hollerith, J. Zeiher, D. M. Stamper-Kurn, C. Gross, and I. Bloch, A subradiant optical mirror formed by a single structured atomic layer, Nature (London) **583**, 369 (2020).
[70] Data for: Theoretical study of early-time superradiance for atom clouds and arrays, https://doi.org/10.4231/CAFS-9A27.
[71] E. Sierra, S. J. Masson, and A Asenjo-Garcia, Dicke superradiance in ordered lattices: Role of geometry and dimensionality, arXiv:2110.08380.